Research article

Functionalized magnetic lipase/Cu$_3$(PO$_4$)$_2$ hybrid nanoflower: Synthesis, characterization, and enzymatic evaluation

Shamini Anboo [a], Sie Yon Lau [a,*], Jibrail Kansedo [a], Pow-Seng Yap [b], Tony Hadibarata [a], Azlina Harun Kamaruddin [c]

[a] Department of Chemical Engineering, Faculty of Engineering and Science, Curtin University Malaysia, CDT 250, 98009, Miri, Sarawak, Malaysia
[b] Department of Civil Engineering, Xi'an Jiaotong-Liverpool University, Suzhou, 215123, China
[c] School of Chemical Engineering, Universiti Sains Malaysia, 14300, Nibong Tebal, Seberang Perai Selatan, Penang, Malaysia

ARTICLE INFO

ABSTRACT

This paper reports the synthesis of magnetic lipase/Cu$_3$(PO$_4$)$_2$ hybrid nanoflowers via a rapid ultrasonication method. The enzyme immobilization and nanoflower growth mechanism can be described as the (a) Fe^{2+}, Cu^{2+}, and phosphate "binding", (b) metal phosphate crystals formation, (c) formation and growth of metal phosphate crystals to form plate-like structures, and (d) self-assembly of plate structures that forms a flower-like structure. Some factors contributing to the morphology of the hybrid nanoflowers structure includes the time and concentration of lipase were studied. The effect of temperature, pH, and duration on the enzyme immobilization yield were also studied. In addition, the strong magnetic property (9.73 emu g^{-1}) of the nanoflowers resulted in higher retrievability and reusability after repeated usage. Furthermore, the catalytic activity of lipase/Cu$_3$(PO$_4$)$_2$ hybrid nanoflowers was investigated and the ideal conditions were determined whereby, the maximum activity was calculated to be 1511 $\pm$ 44 U g^{-1}, showing a catalytic enhancement of 89% in comparison to free lipase. The reusability study showed that, after 5 cycles, the magnetic lipase/Cu$_3$(PO$_4$)$_2$ nanoflowers successfully retained 60% of its initial activity. From the results obtained, it is worth noting that, the magnetic lipase/Cu$_3$(PO$_4$)$_2$ hybrid nanoflowers are highly efficient in industrial biocatalytic applications.

1. Introduction

Over the past decade, enzyme immobilization technique has been incorporated into nanostructures to act as platforms to promote higher efficiency, and storage stability of enzymes which enhances their reusability value and ultimately becomes more economically efficient in comparison to free enzymes [1–5]. The attachment of enzymes onto a platform and/or support is known as the process of enzyme immobilization [6]. This process is often accomplished through physical and/or chemical bonding. The physical bonding methods include adsorption or entrapment whereas, chemical bonding is through a covalent bonding or cross-linking [7]. Immobilized enzymes sometimes may show reduced activity in the case of the (a) type of organic solvent used immobilized parts of the enzyme, (b) active site of enzyme is blocked which reduces availability, (c) support matrix that acts as an inhibitor, and (d) mass transfer between enzyme and substrate [8–12]. This shows that there is room to improve current immobilization methods to increase stability, longevity, and catalytic performance of immobilized enzymes.

---

* Corresponding author.
  E-mail address: johnlsy@curtin.edu.my (S.Y. Lau).

The breakthrough from Ge et al. (2012) involving the synthesis of copper sulphate as an inorganic component and bovine serum albumin as an organic component revolutionized the development of protein-inorganic hybrid nanoflowers (NFs). The study showed that immobilized enzymes had higher enzymatic activity than free enzymes by ~650% [13]. Zhang et al. [14] prepared lipase/$Zn_3(PO_4)_2$ hybrid NFs using a facile one-step precipitation method inspired by previous studies [13–15]. The study showed that the enzymatic activity of the immobilized enzyme had increase by 147% compared to free lipase [14]. A more recent study showed that lipase immobilized using the co-precipitation method onto magnetic NPs had an enhancement of 189.6% [16], meanwhile Anboo et al. (2023) showed a 90.5% enhancement when lipase was immobilized onto copper phosphate NFs [17]. Several reasons why immobilized enzymes have a significantly high enzymatic activity is because of the: (i) interaction and bonding mechanism between enzyme and inorganic component, (ii) hybridizing effect which creates an allosteric effect of the immobilized enzymes and (iii) large surface area due to the flower-like structure [14].

The development of protein inorganic hybrid nanoflower developed by Batule et al. [18] sparked researchers as the method of synthesis is one-step, fast, green and requires low energy consumption. The method only requires a sonication time of 5 min at room temperature, which drastically reduced the preparation time. The enzymes chosen in the study were laccase and bovine serum albumin. The study also revealed that longer duration of synthesis (7 min) had slight or no impact on the growth of the NFs. There were no significant changes in the morphology and arrangement of the hybrid NFs unlike the change in enzyme loading. Higher enzyme concentrations yielded in a more irregular structure due to agglomeration of enzymes [18].

Inspired and modified as seen fit by the previous studies, herein, we select $CuSO_4$ as primary inorganic component and lipase as the organic component to develop magnetic lipase/$Cu_3(PO_4)_2$ hybrid NFs. In comparison to other metal ions, copper is a common metal ion primarily used in various studies due to its catalytic property, is readily available, and cheap. Lipase was chosen because of its sensitivity to hydrophilic and hydrophobic characteristics on carrier/support due to interfacial activation [13]. The main objective of this paper is the mechanistic study of magnetic lipase/$Cu_3(PO_4)_2$ hybrid NFs using a facile one-step ultrasonication method as well as to analyse the effect of varying parameters and the inorganic components used during synthesis through material characterization. The experiment was based on the formation and bonding mechanism of the hybrid NFs which is illustrated below. The formation and bonding mechanism was studied by altering duration of synthesis and concentration of lipase to observe the change in particle size and definition of the NF architecture. Several other influencing factors on the morphology, arrangement, properties, enzyme loading capacity and catalytic activity of synthesized hybrid NFs were also investigated.

2. Experimental sections

2.1. Material and chemical preparations

Lipase from porcine pancreas, phosphate buffered saline (PBS), bovine serum albumin (BSA), hydrochloric acid (HCl), and Triton-X were purchased from Sigma-Aldrich (M) Sdn. Bhd. Whereas, copper (II) sulphate pentahydrate ($CuSO_4 \cdot 5H_2O$), iron (II) sulphate heptahydrate ($FeSO_4 \cdot 7H_2O$) and sodium hydroxide (NaOH) were purchased from regional representation, Merck Sdn. Bhd. Bradford reagent (1-1400 $\mu g\ mL^{-1}$ protein) was purchased from Supelco. Cupric acetate pyridine reagent (CAPR) was prepared by mixing cupric acetate monohydrate ($Cu(CO_2CH_3)_2 \cdot H_2O$) and pyridine (purchased from Sigma-Aldrich (M) Sdn. Bhd.) until pH 6 was achieved. The olive oil used for enzymatic activity was purchased from local grocery store. All reagents were analytical and pure.

2.2. Synthesis of magnetic Lipase/$Cu_3(PO_4)_2$ hybrid NFs

The experimental procedure was inspired and modified from the works of Batule et al. [18]. 0.2 M aqueous copper (II) sulphate solution and 0.2 M iron (II) sulphate solution in the volume ratio of 1.5:1 was added to 3 M NaOH until pH 11–12 was achieved. Equations (1)–(6) shows the sonochemical formation of magnetite [19].

$$H_2O \rightarrow H \bullet + OH \tag{1}$$

$$H \bullet + H \bullet \rightarrow H_2O \tag{2}$$

$$OH \bullet + OH \bullet \rightarrow H_2O_2 \tag{3}$$

$$FeSO_4\ (s) \rightarrow Fe^{2+}\ (aq) + (SO_4)^{2-}\ (aq) \tag{4}$$

$$2Fe^{2+} + H_2O_2 \rightarrow 2Fe^{3+} + 2OH^- \tag{5}$$

$$Fe^{2+}\ (aq) + Fe^{3+}\ (aq) + 8OH^-\ (aq) \rightarrow Fe_3O_4\ (s) + 4H_2O \tag{6}$$

The precipitate was collected, neutralized to pH 7.2 before adding to 3 mL of phosphate buffer solution of pH 7.2 at room temperature. Lipase was added to the mixture in order to obtain a concentration of 0.3 mg mL^{-1}. The mixture was then ultrasonicated at 30 °C using distilled water in ultrasonic cleaner (6L, Cole-Parmer) operating at 40 kHz powered at 150 W for 7 min. Upon sonication, the obtained solution was centrifuged at 3600 rpm for 6 min (Universal 320R, Hettich). The precipitate was collected and freeze-dried for further analysis.

2.3. Characterization of magnetic Lipase/Cu₃(PO₄)₂ hybrid NFs

The average particle diameter and size distribution of magnetic lipase/$Cu_3(PO_4)_2$ hybrid NFs were determined using Light Scattering Particle Size Distribution Analyzer (PSA, LA-960, Horiba Scientific) to improve accuracy, reproducibility, and stability as the equipment is a realignment-free operation. The testing system was ultrapure water (25 °C, refractive index 1.529). Fourier Transform Infrared (FTIR) spectra was determined using FTIR microscope fitted with attenuated total reflection (ATR) detector and diamond crystal (Cary 630, Agilent Technologies). The measurements were obtained by scanning each sample between 4000 and 600 cm^{-1} wavenumbers. The morphology, supramolecular arrangements, and elemental compositions were observed using Scanning Electron Microscope and Energy Dispersive X-Ray respectively (SEM, Quattro S, Thermo Scientific). Magnetisation study was analyzed using Vibrating Sample Magnetometer (VSM, LakeShore 340, Lakeshore Cryotronics) whereby the magnetic field used was between -8kOe to +8 kOe at room temperature. The crystalline properties of the magnetic hybrid nanoflowers (mhNFs) were studied using an X-Ray diffraction (XRD, MiniFlex, Rikagu) technique in a 2θ ranging from 10° to 90° with step size of 0.01 s and step time of 1 s with close reference to previous study [20]. The zeta potential was studied using a zeta sizer (ZEN3600, Malvern Zeta sizer Nano ZS) whereby, the magnetic lipase/$Cu_3(PO_4)_2$ hybrid NFs were dispersed in PBS solution of various pH ranging from 2 to 14 to determine the isoelectric point at room temperature and refractive index of 1.8. The zeta potential of pure $Cu_3(PO_4)_2$ and Fe_3O_4 magnetite NPs were also included for comparison purposes. The formation and bonding mechanism was experimented by changing concentration of lipase and duration of synthesis to observe the change in particle size as well as definition of the NF architectures.

2.4. Enzymatic activity of magnetic Lipase/Cu₃(PO₄)₂ hybrid NFs

The enzymatic activity was studied using olive oil substrate emulsion from the works of Mustafa et al. [21] with minor modifications. Firstly, an olive oil substrate emulsion was formed by mixing olive oil, 1% (v/v) Triton-X, and PBS (pH 8) in the ratios of 2:1:1 v/v respectively. The mixture was let to emulsify with gentle stirring before adding 20 mg of magnetic lipase/$Cu_3(PO_4)_2$ hybrid NFs and incubated at 37 °C at 150 rpm for 40 min 0.5 mL of samples were taken out every 10 min to allow reaction with 0.6 mL of CAPR
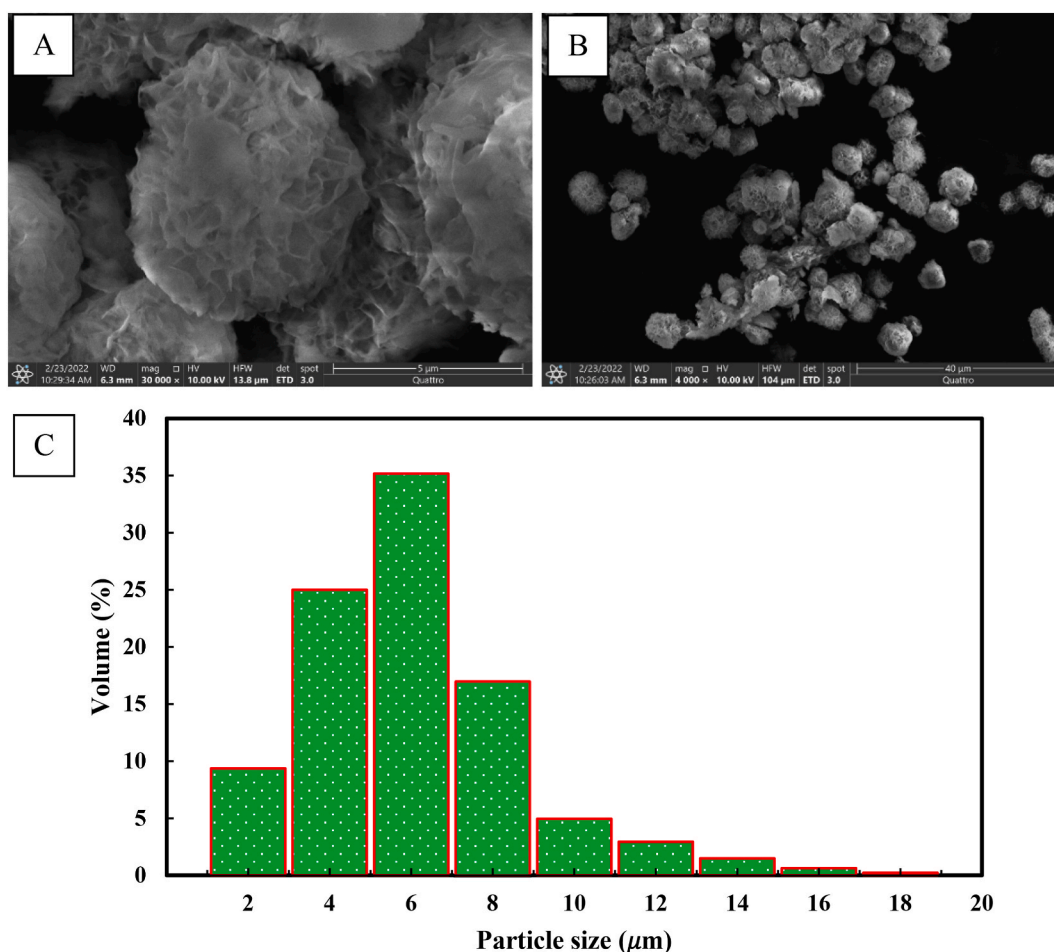
Fig. 1. SEM images of magnetic lipase/$Cu_3(PO_4)_2$ hybrid NFs (A–B); Size distribution of magnetic lipase/$Cu_3(PO_4)_2$ hybrid NFs (C).

and 2.5 mL of hexane. The solution was allowed to mix through a micropipette whereby, the solvent was collected and then released to ensure the solution was well mixed. The purpose of adding hexane is to ensure the fatty acid soaps dissolve before analysis. Finally, 500 μ L of the blueish-green solution was taken out and analyzed using a UV–vis spectrometer (DR-2800, HACH) at an absorbance of 655 nm. Progress curves were plotted to evaluate the enzymatic activity of lipase, whereby, oleic acid was used as standard solution. The immobilization yield was calculated by measuring the protein concentration in supernatant upon centrifuging the solution using Bradford assay and BSA as standard solution. Triplicate readings was measured using UV–vis spectrometer at 595 nm.

$$\text{Activity enhancement} = \frac{\text{rate of enzymatic activity of immobilized lipase}}{\text{rate of enzymatic activity of free lipase}} \times 100\%$$

$$\text{Immobilization yield} = \left(1 - \frac{\text{remainder lipase}}{\text{initial lipase}}\right) \times 100\%$$

2.5. Stability and reusability analysis

The thermal, pH, and storage stability of magnetic lipase/$Cu_3(PO_4)_2$ hybrid NFs and free lipase were also conducted. The pH stabilities of magnetic lipase/$Cu_3(PO_4)_2$ hybrid NFs were determined in the range of 3, 5, 7.2, 9, and 11, ranging from an acidic to an alkaline environment. The pH was adjusted by the addition of HCl and NaOH for acidic and alkaline conditions respectively. The thermal stability was conducted in the range of 30–50 ° C with an increment of 10 ° C, whereas, the storage stability was studied by evaluating enzymatic activity for 20 days whereby, the residual activity was measured every 2 days. The enzyme activity was studied using the assay described above unless specified. Triplicate readings was measured.

3. Results and discussion

3.1. Morphology of magnetic Lipase/$Cu_3(PO_4)_2$ hybrid NFs

Precipitates of different colors were collected for further analysis and characterization. The series of colored precipitates include blue and dark brown to black for lipase/$Cu_3(PO_4)_2$ and magnetic lipase/$Cu_3(PO_4)_2$ hybrid NFs respectively. Based on previous reported study [17], the pure $Cu_3(PO_4)_2$ NPs show sharp and spiky-edged structures which further enhances the orifices and prevents clogging. The SEM images of enzyme-incorporated hybrid NFs are presented in Fig. 1A and B. The synthesized magnetic lipase/$Cu_3(PO_4)_2$ hybrid NFs exhibited beautiful, homogenous flower-shaped structures with high surface-to-volume ratio as the edges of the stellate are sharp and distinctive. This suggests that the nanoflower structure was formed through the stacking of numerous nanoplates also known as the "petals" of the hybrid NF structures. The presence of nanoplates and the significant clearance between them resulted in the high surface area and porosity [14].

Fig. 1C shows the particle size distribution of magnetic lipase/$Cu_3(PO_4)_2$ hybrid NFs using dynamic light scattering (DLS) whereby, the smallest particle size is 2.7 μ m and average particle size is 5.76 μ m which is in fair agreement with the SEM analysis and previous reported works [18,22,23].
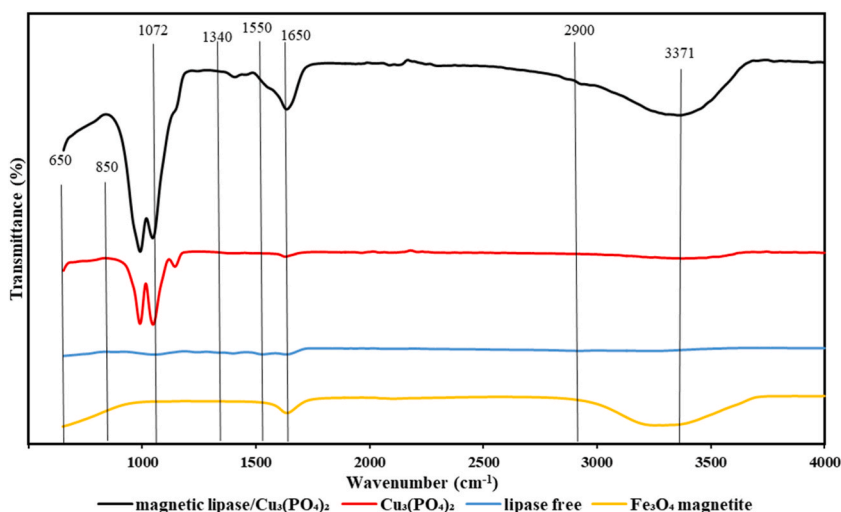

Fig. 2. FTIR spectra: free lipase, $Cu_3(PO_4)_2$, Fe_3O_4 magnetite and magnetic lipase/$Cu_3(PO_4)_2$ hybrid NFs.

3.2. Components and properties of magnetic Lipase/Cu$_3$(PO$_4$)$_2$ hybrid NFs

The composition and properties of prepared magnetic lipase bound hybrid NFs was studied using infrared spectrum to systematically analyse the samples. Fig. 2 shows the FTIR spectra of various samples including free lipase, Cu$_3$(PO$_4$)$_2$, and magnetic lipase/Cu$_3$(PO$_4$)$_2$ to analyse the difference in peaks and functional groups present.

From Fig. 2, it can be seen that the hybrid NFs incorporates the main absorbance spectra of free lipase as well as Cu$_3$(PO$_4$)$_2$ particles. Peaks observed between 1650 cm^{-1}, 1350 cm^{-1}, 1460 cm^{-1} and 1020-1220 cm^{-1} are typical protein and/or enzyme characteristics [24]. Free lipase typical peaks include peaks between 1650 and 1550 cm^{-1} –CONH and 2800–3000 cm^{-1} for CH$_2$ and CH$_3$ bonds [25]. It can be observed that the hybrid magnetic NFs share similar peaks. It also has sharper peaks which may be due to the interaction between amino groups on lipase and the inorganic component. The peak at 3371 cm^{-1} indicates the potential coordination between the Fe^{2+}, Cu^{2+}, and amino groups present on lipase with close reference to Zhang et al. (2016) [14]. In addition, P–O stretching between 1072 cm^{-1} and 850 cm^{-1} indicates the relationship between phosphate groups within the hybrid NFs' structure [26]. It is also noteworthy that no significant shifts between peak positions were observed.

The elemental composition study was conducted as shown in Figs. 3 and 4. The EDX analysis showed the common elements attributed to magnetic lipase/Cu$_3$(PO$_4$)$_2$ hybrid NFs including Cu, Fe, P, O, N, and C. The mapping of magnetic lipase/Cu$_3$(PO$_4$)$_2$ shows that the elemental composition is made up of elements combined from free lipase and pure Cu$_3$(PO$_4$)$_2$ NPs as shown in Fig. 3A–C. The complete elemental compositional analysis is shown in Fig. 4A–C whereby, it was performed using energy dispersive spectroscopy by measuring intensity and energy distribution of X-ray signal generated when the electron beam strikes the surface of the specimen. It is notable that, the weight percentage of carbon in Fig. 4A is the highest with respect to the pure Cu$_3$(PO$_4$)$_2$ NPs and mhNFs due to specimen being pure lipase without added inorganic component and/or impurities from the metal salts. Pure Cu$_3$(PO$_4$)$_2$ NPs also have higher weight percentage of cupper than mhNFs whereby, the results are similar to the FTIR spectrum in Fig. 2 and previous studies using similar components [27,28].

The magnetic properties of the hybrid NFs synthesized can be proven as shown in Fig. 5A and B. The addition of NaOH allowed for the formation of Fe$_3$O$_4$ magnetite which carries the magnetic properties. The magnetic lipase hybrid NFs were dispersed in distilled water and allowed to settle before applying a magnetic field. When the magnetic field was applied using a magnetic stirrer bar, the magnetic enzyme-incorporated hybrid NFs were attracted to the walls of the microvial within 10 s as shown in Fig. 5A. Fig. 5B shows the hysteresis curves of the magnetic lipase hybrid NFs developed. The magnetic hysteresis curves are S-shaped loops whereby, all of the loops shows negligible coercivity and remanence proving the superparamagnetism characteristics [29–31]. The magnetisation of
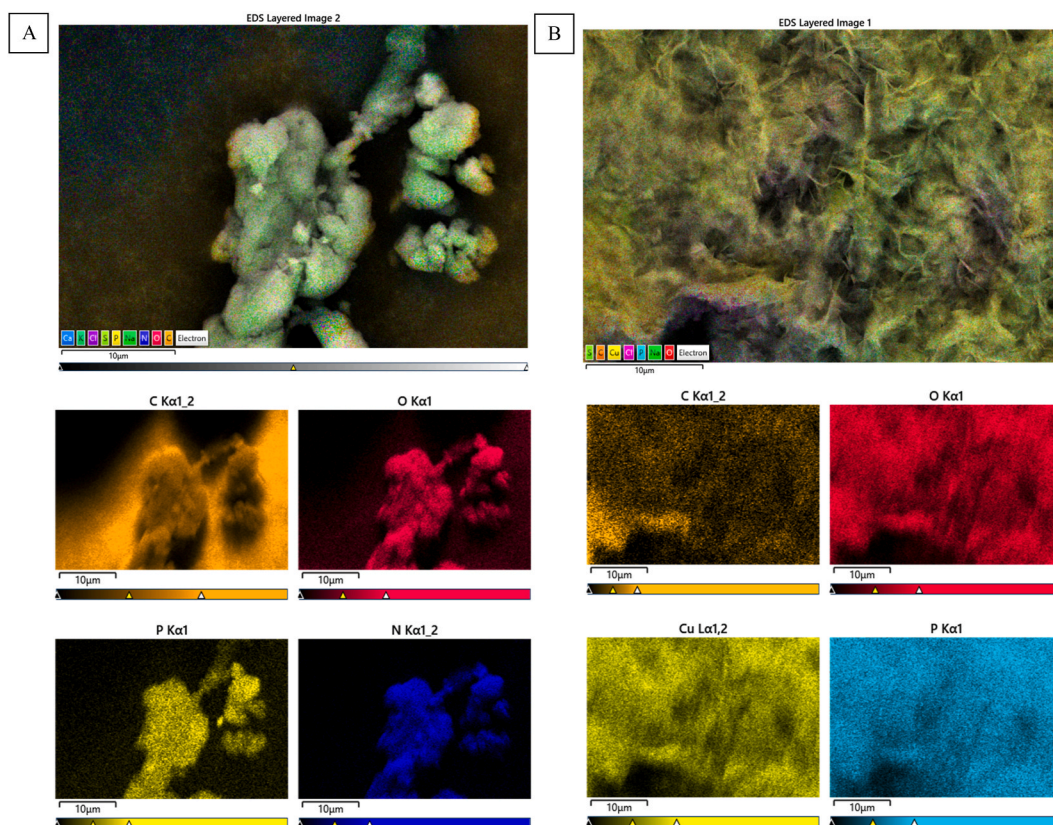

Fig. 3. Elemental composition by element: free lipase (A); pure Cu$_3$(PO$_4$)$_2$ NPs (B), and magnetic lipase/Cu$_3$(PO$_4$)$_2$ hybrid NFs (C).
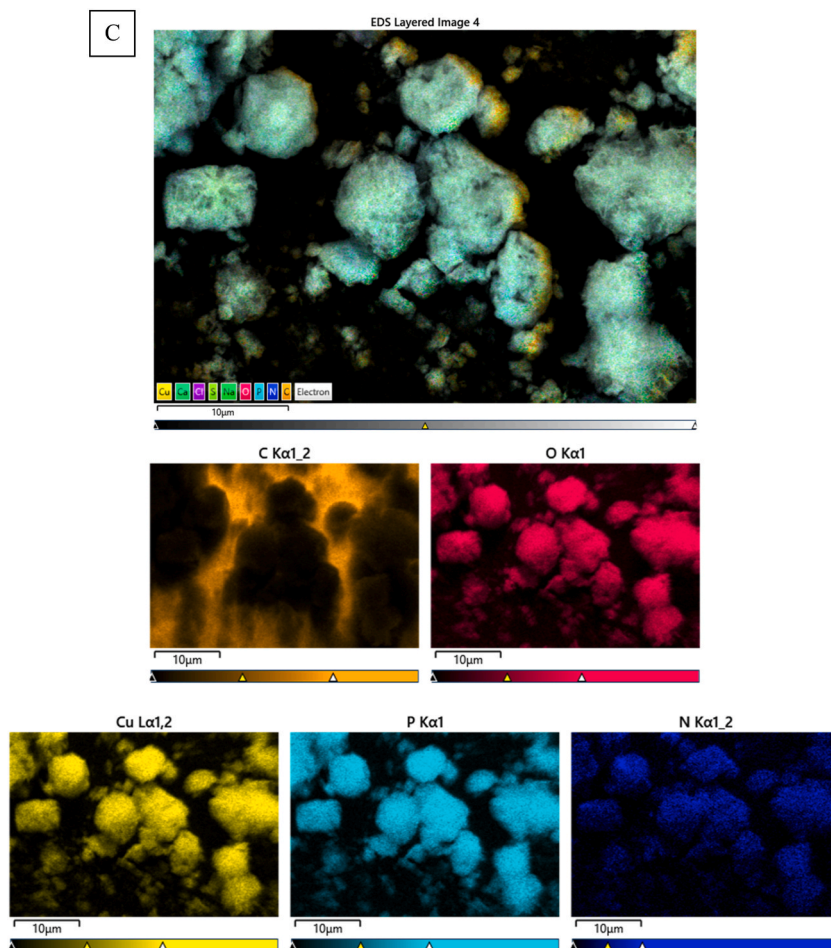
C

Fig. 3. (*continued*).

magnetic lipase/$Cu_3(PO_4)_2$ hybrid NFs were 9.73 emu g^{-1}. The magnetic lipase/$Cu_3(PO_4)_2$ hybrid NFs showed a higher magnetisation than previous reported work with magnetisation values of 7.51 emu g^{-1} [29] and 8.159 emu g^{-1} [16]. It can be suggested that various factors: (a) the method of preparation, (b) the combination of inorganic components, and (c) the operating conditions affected the magnetisation values.

The X-ray diffractogram patterns of free lipase, $Cu_3(PO_4)_2$ NPs, and various mhNFs are shown in Fig. 6. From the figure, we can observe free lipase had pronounced peaks at $2\theta = 12°$, $16°$, $20°$, $21°$, and $24°$ which is in agreement with previous study [14]. $Cu_3(PO_4)_2$ NPs had significant peaks at $2\theta = 13°$, $32°$, $36°$, $45°$, $56°$, and $75°$ which matches with little discrepancy with the standard $Cu_3(PO_4)_2 \cdot 3H_2O$ XRD pattern (JCPDS: 22–0548). The XRD pattern of magnetic lipase/$Cu_3(PO_4)_2$ NFs contain the diffraction peaks and crystalline compounds of free lipase and $Cu_3(PO_4)_2$ NPs. Aside from that, the magnetic lipase/$Cu_3(PO_4)_2$ NFs contain significant peaks at $2\theta = 32°$, $35°$, $47°$, $62°$, and $67°$ which is highly likely to be contributed by the magnetic component, Fe_3O_4 magnetites as assigned (JCPDS: 01-071-6336) [32]. Thus, the inorganic component of magnetic lipase/$Cu_3(PO_4)_2$ NFs were copper phosphate pentahydrate and iron (II, III) oxides.

Zeta potential is a physical property typically exhibited by particles in suspension. The analysis is done to understand and predict the long-term stability of particles. In this case, the zeta potential analysis can aid in the formulation of protein solutions and its interaction in dispersant solutions [33]. Colloidal system of hybrid NFs can be defined as the dispersion of solid hybrid NFs in PBS, dispersant solution. Colloidal stability can be described as the degree of flocculation, whereby, if the particles have high repulsion from one another, the degree of flocculation is lower, hence, increasing colloidal stability [34]. In order to achieve colloidal stability, the electrostatic or charge stablization must be achieved, whereby, the charge distribution effects the particle interaction. The electrostatic stabilization mechanism typically involves the altering of concentration of positive or negative ions in dispersant [35]. The mechanism of electrostatic stabilization of NPs in dispersant solution is when the van der Waals forces are balanced with electrostatic repulsion as similar charges group on the external layer of particles which ultimately leads to a steric repulsion to achieve colloidal stability. The key advantage of this mechanism is it is reversible and cheap.

The zeta potential of the magnetic lipase/$Cu_3(PO_4)_2$ hybrid NFs can be shown in Fig. 4.4B–C. The magnitude of zeta potential shows the collodal stability of the particles, whereby a high positive or negative value means a high repulsion and low degree of flocculation
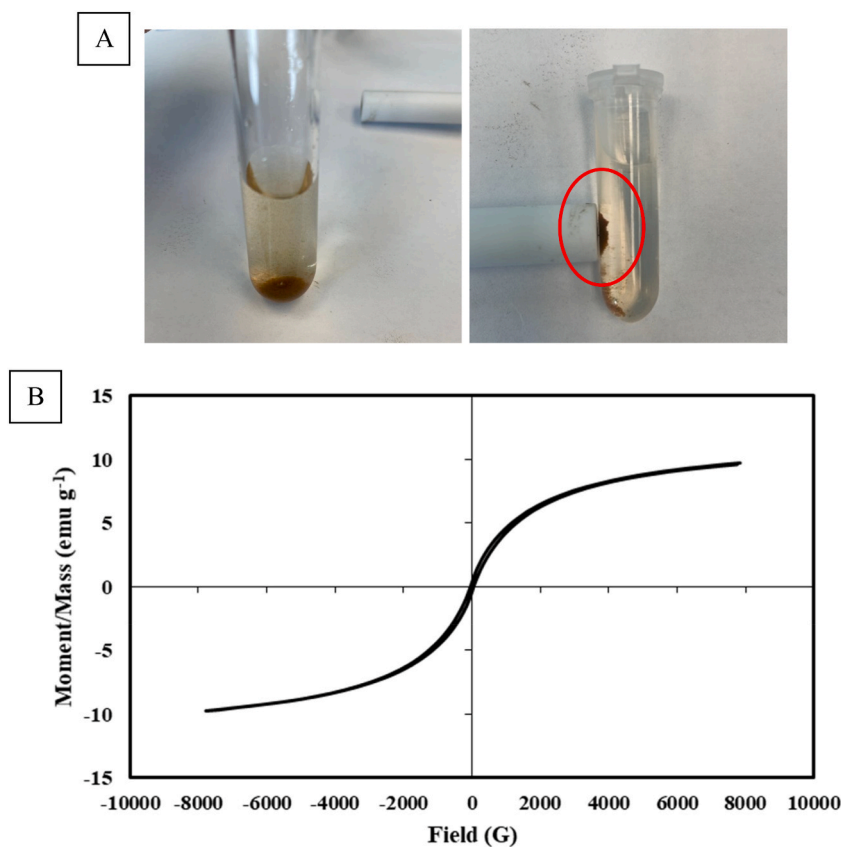
Fig. 4. Complete elemental composition: free lipase (A); pure $Cu_3(PO_4)_2$ NPs (B), and magnetic lipase/$Cu_3(PO_4)_2$ hybrid NFs (C).

[34,36]. From Fig. 7, we can observe the effect of pH on the zeta potential on the colloidal stability of the hybrid NFs in dispersant. As the particles are dispersed in a more acidic environment, the high number of positively charged ions causes the zeta potential to be higher than +5 mV, whereas as the pH increases, the particles approaches a larger negative zeta potential value. Fe_3O_4 magnetites had a larger zeta potential (−25 mV) value in comparison to pure $Cu_3(PO_4)_2$ NPs and magnetic lipase/$Cu_3(PO_4)_2$ hybrid NFs, ~ −16 mV. This may be due to the interaction between amino groups on protein bound hybrid NFs which shifts the overall colloidal stability. The point where the plot crosses the x-axis is known as the isoelectric point (zeta potential = 0 mV). The isoelectric point is normally the most unstable point whereby, aggregation is highest causing particles to flocculate making the system lose its stability [36]. Therefore, we can conclude that all systems are least stable at around pH 3–3.5 and increases in stability when pH is greater than 7.

3.3. Formation and bonding mechanism of magnetic Lipase/$Cu_3(PO_4)_2$ hybrid NFs

In order to investigate the bonding and formation process of the hybrid NFs in extensive, the morphology of the samples synthesized at different time intervals were conducted and observed. Fig. 8A–D shows the formation of magnetic lipase/$Cu_3(PO_4)_2$ hybrid NFs at different time intervals to investigate the formation and growth of nanostructures. The SEM images show that the nanostructures have not fully developed at lesser growth periods (t = 1 min and 5 min). The architectures of the samples consist of agglomerated lipase and under developed metal phosphate crystals. The nanoplate "petals" clearly did not have sufficient time to grow and develop into a full bloom flower-like structure unlike at time, t = 7 min. At t = 7 min, the overall structure's thickness and particle size increased indicating the particle was growing. The particle size analysis was also conducted in order to analyzed the size increment whereby, magnetic lipase/$Cu_3(PO_4)_2$ hybrid NFs were synthesized at different time intervals from time, t = 0 to t = 10 min ±1 min. Fig. 8E shows the particle size increment until the particle curve falls at time, t = 10 min, conforming that the particle does not grow any further which aligns with the outcomes from previous study [18].

From the above results, the possible formation is proposed, as shown in Fig. 9. Firstly, Fe^{2+}, Cu^{2+}, and phosphate "binding" occurred in simultaneous to the "binding" between Cu^{2+} ions and lipase [13,14,37,38]. Copper phosphate crystals and

Fig. 5. Magnetic attraction between magnetic hybrid NFs and magnet: before *(right)* and after *(left)* (A); Hysteresis curve of magnetic lipase/Cu$_3$(PO$_4$)$_2$ hybrid NFs (B).
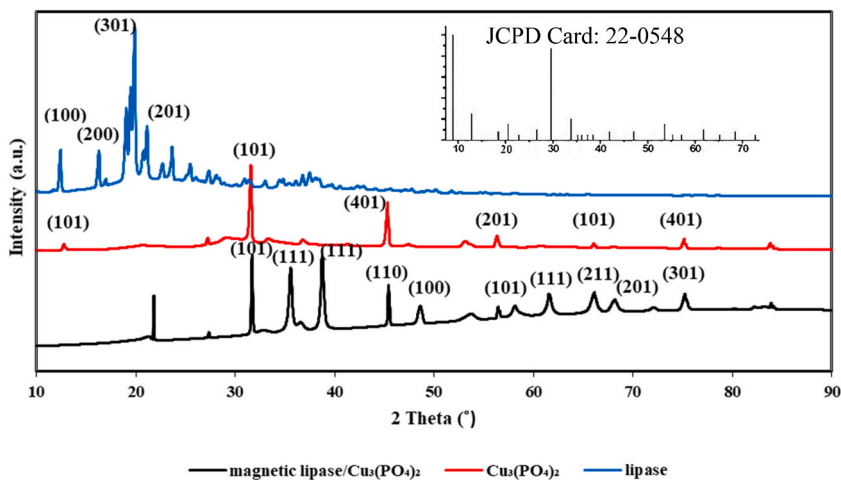

Fig. 6. X-Ray diffractogram patterns: free lipase, Cu$_3$(PO$_4$)$_2$ and magnetic lipase/Cu$_3$(PO$_4$)$_2$ hybrid NFs.

lipase/Cu^{2+}/Fe^{2+} hybrid particles resulted as products from the above mechanism. The formation and growth of metal phosphate crystals to form plate-like structures resulted from lipase being a precursor. Self-assembly between these plate structures finally resulted in the formation of well-designed magnetic lipase/Cu$_3$(PO$_4$)$_2$ hybrid NF structure.
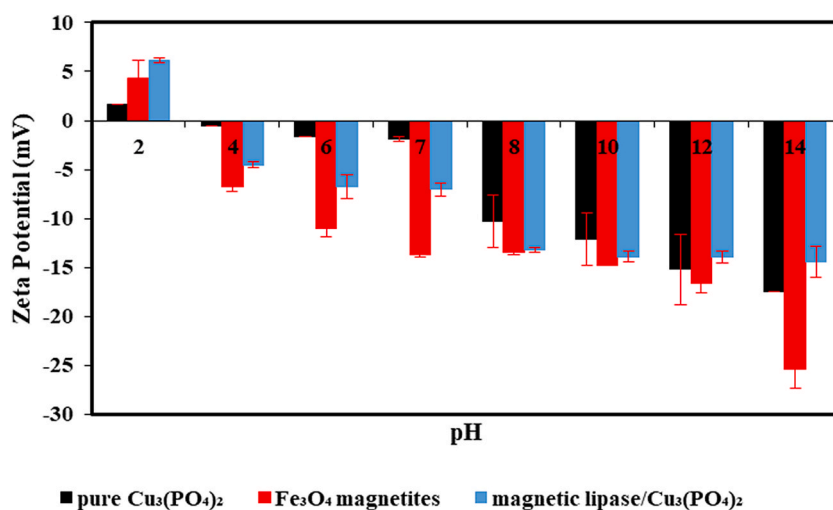
Fig. 7. Effect of pH on the zeta potential of various samples

3.4. Controlled integration of magnetic Lipase/Cu₃(PO₄)₂ hybrid NFs

In order to study the effect of adding lipase on the morphology and distribution of hybrid NFs, different initial concentrations of lipase were added during synthesis. The lipase concentration that was used ranged between 0.1 and 0.5 mg mL^{-1}. Increasing the concentration from 0.1 to 0.3 mg mL^{-1} showed that the nanoplates were able to stack well and form a beautiful flower-like hybrid NF structure. The plates also had sharp prominent edges and a uniform architecture between each particle in comparison to the 0.1 mg mL^{-1} lipase concentration, as shown in Fig. 10A and B. This may be due to the lack of precursors for the crystals to be able to grow and fully develop. A further increase in lipase concentration to 0.5 mg mL^{-1}, the structure became more agglomerated and lacklustre as the edges of the hybrid NFs lost its flower-like architecture and looked like a non-uniform crystalline structure as shown in Fig. 10C. This is because the lipase acted as a surface inhibitor in the formation of metal phosphate crystals and soon after, the stacking and arrangement of nanoplates leading to the flower-like structure [14].

3.5. Immobilization yield study of magnetic Lipase/Cu₃(PO₄)₂ hybrid NFs

The immobilization yield of magnetic lipase/Cu₃(PO₄)₂ hybrid NFs have shown to vary across different operating conditions as shown in Table 1. The immobilization yield was calculated to be 97.8% with an actual enzyme loading of 0.293 mg mL^{-1} under standard operating conditions.

Fig. 11 shows the trend of immobilization yield across samples 1 to 19. The average yield across all 19 samples were calculated to be 85.4%. From the results obtained, as temperature increases, the yield increases which then eventually drops. The initial increase in yield is due to the increase in enzyme molecule vibrations due to higher kinetic energy [39], however, as the temperature was further increased $\geq 40\,^\circ$C, the yield drops as the extreme temperatures may have limited the kinetic activity of lipase.

As for the effect of varying concentrations of lipase, at lower concentrations, (0.1–0.2 mg mL^{-1}) the yield is also considerably lower because there is essentially lesser lipase to act at precursors for immobilization to occur as seen from the yields of sample 6 and 7 (25.3% and 62.2%) respectively. The lipase concentration of 0.3 mg mL^{-1} showed the highest immobilization yield (97.8%) meanwhile dropping consistently as the concentration was further increased to 0.5 mg mL^{-1}. This may be due to the higher concentrations of lipase that causes the lipase molecules to agglomerate and reduce enzyme-enzyme interactions interrupting the coordination between the lipase and inorganic ions.

The effect of acidic and alkaline environment on the immobilization yield varied. Between acidic (pH 3 and 5) and alkaline environment (pH 9 and 11) the immobilization yield study showed a lesser yield compared to pH 7.2. The variation in presence of cations, H+ in acidic conditions and anions, OH- in alkaline conditions may have played a role in the differing yields. In a previous study by Arana-Peña et al. (2020), it was found that phosphate anions negatively impacted the immobilization yield and enzyme stability [40]. Therefore, it can be suggested that, at lower pH, with higher H+ ions, ionic bonding neutralized the presence of phosphate anions which resulted in a higher enzyme immobilization yield compared to in an alkaline environment.

Finally, the effect of duration of synthesis on the immobilization yield showed that as the time increased, yield increased. Further increase in the duration (>8 min) showed a smaller yield as seen from sample 18 and 19 (73% and 73.9%) respectively. It can be suggested that the immobilization of lipase was complete at t = 7 min and a further increase in time did not promote for a higher immobilization yield. Sonication produces gas bubbles which collapses through a process called cavitation resulting in the formation of H● and OH● free radicals. Therefore, these free radicals can undergo further reactions (oxidation, cross-linking, cleavage reactions) that ultimately decreases protein stability leading to aggregates [41].
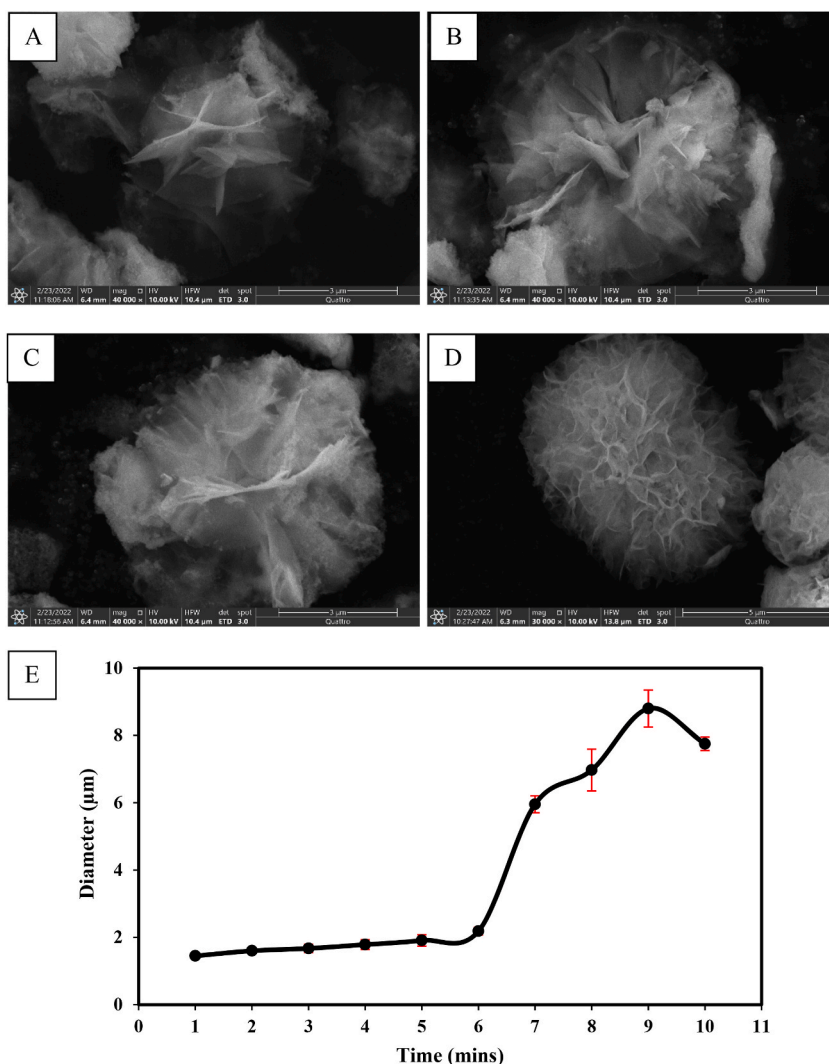
Fig. 8. SEM images of magnetic lipase/Cu$_3$(PO$_4$)$_2$ hybrid NFs under different growing time; 1 min (A); 5 min (B–C); 7 min (D); Particle size increment analysis (E).

3.6. Enzyme activity of magnetic Lipase/Cu$_3$(PO$_4$)$_2$ hybrid NFs

The enzyme activity of magnetic lipase/Cu$_3$(PO$_4$)$_2$ hybrid NFs were found to be 1511 $\pm$ 44 U g^{-1} with an 89% enhancement in comparison to free lipase (166 $\pm$ 3 U g^{-1}) [17] under standard operating conditions. Fig. 12 shows the progress curves of magnetic lipase/Cu$_3$(PO$_4$)$_2$ hybrid NFs and free lipase. The enhanced catalytic activity may have been due to better 3D surface area-to-volume ratio of the magnetic lipase/Cu$_3$(PO$_4$)$_2$ hybrid NFs as well as the synergistic effect between the lipase and inorganic component [14]. Over the years, it was found that the catalytic activity of immobilized lipase has been carefully progressing through various methods and works. For instance one study showed that, lipase immobilized onto calcium phosphate had an activity of 849.8 U g^{-1} [24], whereas another study showed that lipase immobilized onto copper phosphate had an activity of 874.5 U g^{-1} [42] meanwhile Ren et al. (2019) showed that magnetic lipase/Cu$_3$(PO$_4$)$_2$ NFs only had an activity of 92.63 U g^{-1} [29]. A more recent study showed that lipase immobilized using the co-precipitation method onto magnetic NPs had an enhancement of 189.6% [16]. Having said that, the advantage of the method proposed in this study is that, it requires a short synthesis duration and is a far greener method as it does not require any toxic solvents and/or consume high operational energy.

In order to study the effect of varying operating conditions on the relative catalytic activity of magnetic lipase/Cu$_3$(PO$_4$)$_2$ hybrid NFs, the effect of temperature and pH were conducted. The effect of temperature was conducted in the range of 30–50 °C with an increment of 10 °C while maintaining all other parameters constant. The trend lines are shown in Fig. 13A, whereby, it can be seen that as temperatures increased, the overall catalytic activity decreased. This is due to the denaturation of the active sites on enzymes which reduces its ability to carry out catalytic reactions. Nonetheless, the immobilized enzymes had an overall higher activity than free enzymes, whereby, after heating for 6 h at 50 °C, the residual activity of magnetic lipase/Cu$_3$(PO$_4$)$_2$ hybrid NFs were 43.3% which
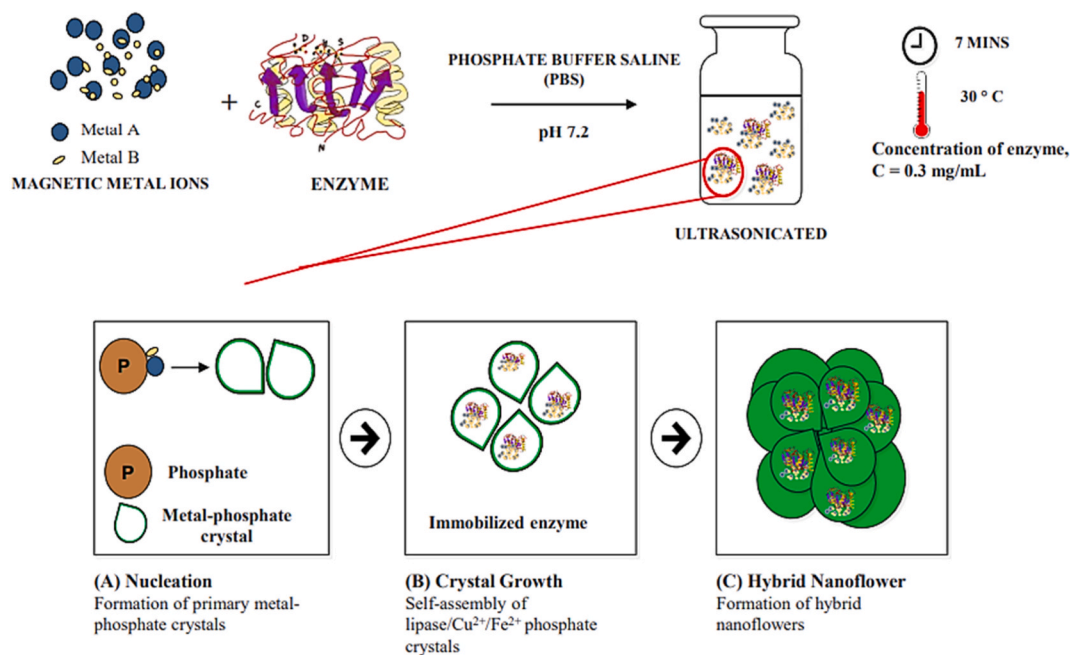
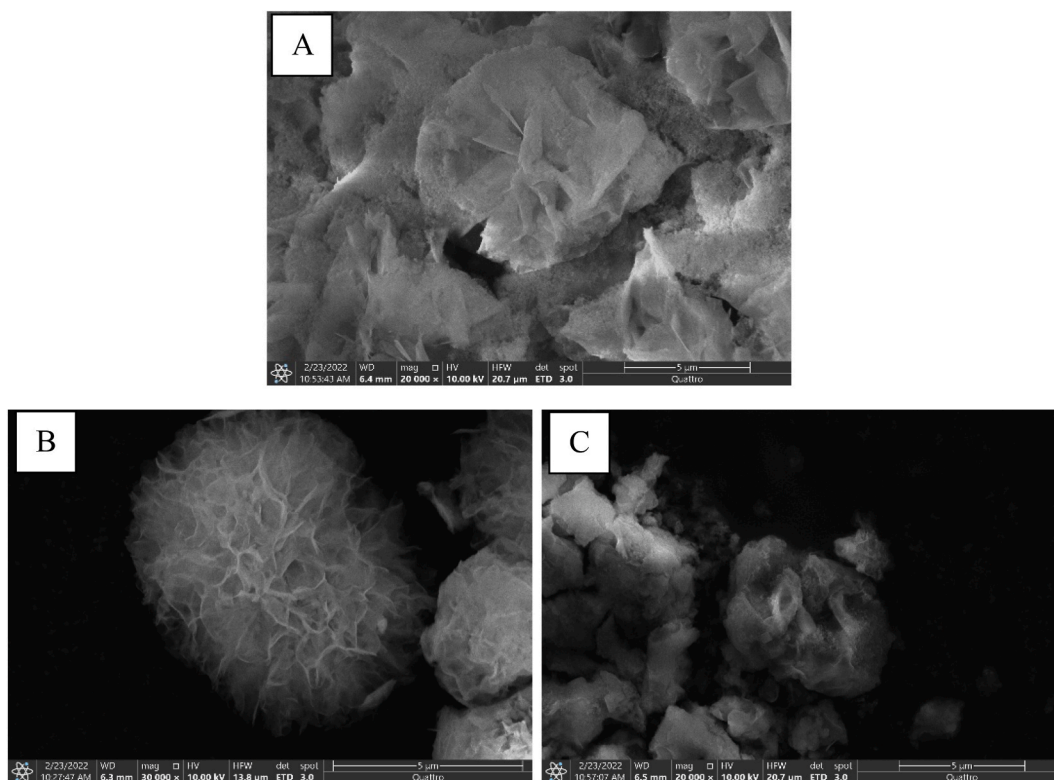**Fig. 9.** Proposed schematic diagram of formation mechanism of magnetic lipase/Cu$_3$(PO$_4$)$_2$ hybrid NFs.

Fig. 10. SEM images of magnetic lipase/Cu$_3$(PO$_4$)$_2$ hybrid NFs synthesized with different concentration of lipase: 0.1 mg mL^{-1} (A); 0.3 mg mL^{-1} (B); 0.5 mg mL^{-1} (C).

Table 1
Varying conditions during synthesis of magnetic lipase/Cu$_3$(PO$_4$)$_2$ hybrid NFs.

Sample no.	Temperature ($^\circ$ C)	Concentration of lipase (mg mL^{-1})	pH	Time (mins)
1	30	0.3	7.2	7
2	35	0.3	7.2	7
3	40	0.3	7.2	7
4	45	0.3	7.2	7
5	50	0.3	7.2	7
6	30	0.1	7.2	7
7	30	0.2	7.2	7
8	30	0.4	7.2	7
9	30	0.5	7.2	7
10	30	0.3	3	7
11	30	0.3	5	7
12	30	0.3	9	7
13	30	0.3	11	7
14	30	0.3	7.2	1
15	30	0.3	7.2	5
16	30	0.3	7.2	6
17	30	0.3	7.2	8
18	30	0.3	7.2	9
19	30	0.3	7.2	10
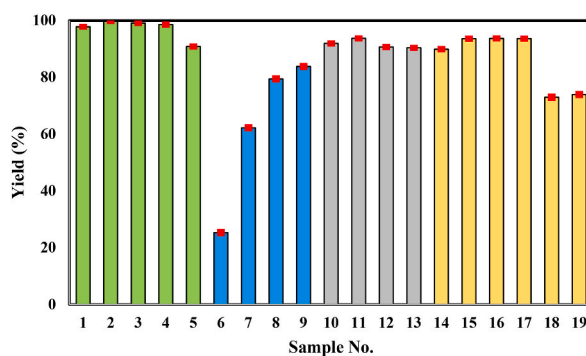
Fig. 11. Trend between immobilization yield and various samples of magnetic lipase/Cu$_3$(PO$_4$)$_2$ hybrid NFs.
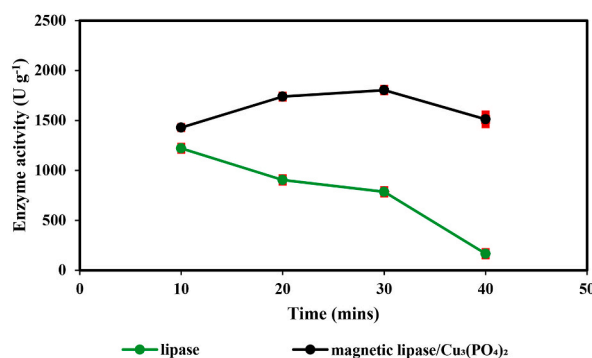

Fig. 12. Enzymatic evaluation of immobilized and free enzymes.

resonates to 8.38 folds to that of free lipase.

The effect of pH on the activity of free and immobilized lipase using olive oil substrate emulsions are shown in Fig. 13B. It was found that, the immobilized enzymes were able to retain most of their catalytic activities across broad pH ranges, whereas the free lipase did not. The ideal pH for both enzymes were pH 7.2. It is noteworthy that, in both cases, the enzymes had a higher relative activity in an acidic environment than alkaline conditions. This is because, at lower pH, with higher H+ ions, the ionic bonding neutralized the presence of phosphate anions resulting in a higher relative activity compared to when it was an alkaline environment. This reasoning can be further justified as Arana-Peña et al. (2020) found phosphate anions negatively impacted the enzyme stability [40].

The storage and operational stability of magnetic lipase/Cu$_3$(PO$_4$)$_2$ hybrid NFs is an important factor in determining the shelf life of
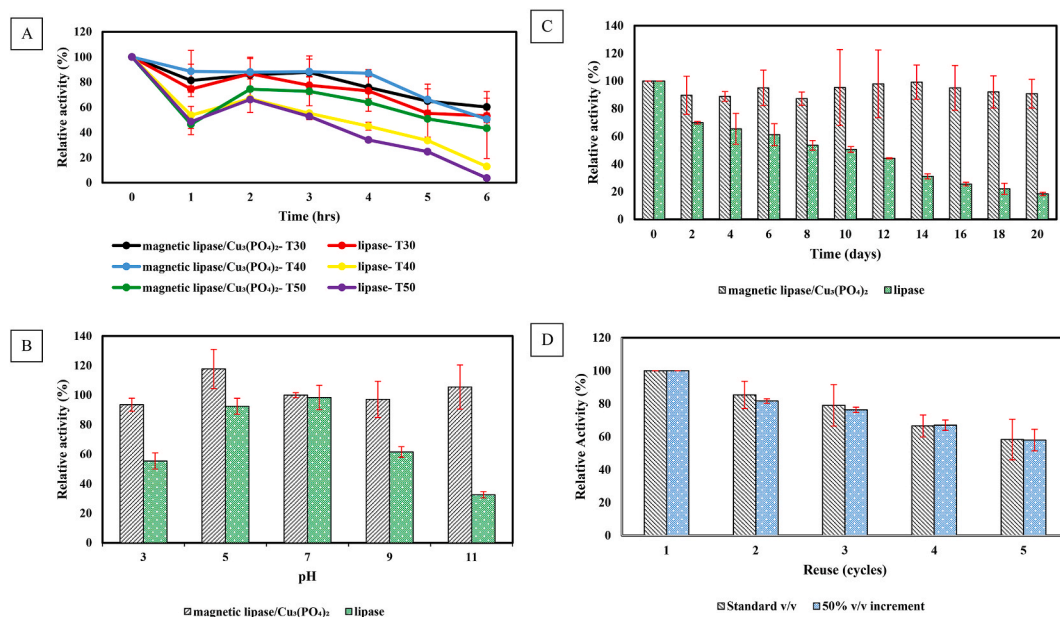
Fig. 13. Effect of temperature (A) and pH (B) on magnetic lipase/Cu$_3$(PO$_4$)$_2$ hybrid NFs and free lipase; Storage stability of magnetic lipase/Cu$_3$(PO$_4$)$_2$ hybrid NFs and free lipase (C); Reusability of magnetic lipase/Cu$_3$(PO$_4$)$_2$ hybrid NFs for hydrolysis of: olive oil substrate emulsion (D).

the magnetic lipase-incorporated hybrid NFs to act as biocatalysts. Therefore, the storage stability of immobilized and free lipase was evaluated as shown in Fig. 13C. From the results obtained, it is notable that the overall storage stability of immobilized lipase is much higher than free lipase. The free lipase lost roughly 82% of its initial activity after the 20-day period in comparison to the immobilized enzyme which only lost 9.3% of its initial activity.

As for the reusability value of magnetic lipase/Cu$_3$(PO$_4$)$_2$ hybrid NFs, it was found that after 5 cycles, the NFs were able to retain about 60% of its initial activity and have successfully retained higher levels of its enzymatic activity and is deemed to have good operational and recyclability value as shown in Fig. 13D. Another emulsion substrate of higher concentration was prepared and used for comparison purpose whereby, the magnetic lipase/Cu$_3$(PO$_4$)$_2$ hybrid NFs were able to retain 58% of its initial activity after 5 cycles as shown in Fig. 13D. Both results show this work produced an averagely high reusability value when compared to previous works that showed 47.7% after 6 cycles [29] and 84% after 10 cycles [16]. This proves the immobilized lipase system can withstand greater concentrations whilst maintaining good operational stability.

4. Conclusion

We have developed an ideal, efficient methodology for the synthesis of magnetic lipase/Cu$_3$(PO$_4$)$_2$ hybrid NFs using the ultrafast sonochemical method. The formation, bonding mechanism, and morphological control have been analytically explored. The morphology of the magnetic lipase/Cu$_3$(PO$_4$)$_2$ hybrid NFs can be altered and optimized by varying the growth time and through the addition of lipase. A shorter growth time prevented the complete development of the NFs whereas, an increased lipase amount created a surface inhibition between the precursors and metal phosphate crystals inhibiting the formation of a flower-like structure. The most ideal conditions for the development of a flower-like structure is a growth time of 7 min and a lipase concentration of 0.3 mg mL^{-1} at 30 $^\circ$ C, and a pH of 7.2. The overall properties of the magnetic lipase/Cu$_3$(PO$_4$)$_2$ hybrid NFs are consistent with functional groups of native lipases further proving the mechanistic formation between the inorganic and organic component. The immobilization yield of magnetic lipase/Cu$_3$(PO$_4$)$_2$ hybrid NFs were calculated to be 97.8%. The effect of varying conditions during synthesis showed the most ideal conditions for the highest immobilization yield were 35 $^\circ$ C, 0.3 mg mL^{-1}, pH 7.2, and duration of 7 min. At time, t = 40 min, the magnetic lipase/Cu$_3$(PO$_4$)$_2$ had a specific enzyme activity of 1511 $\pm$ 44 U g^{-1}, whereby the catalytic enhancement was 89%. Upon studying the effect of temperature and pH, the most ideal conditions was found to be 30 $^\circ$ C and pH 5 whereby the residual activity was maintained above 80%. The magnetic lipase/Cu$_3$(PO$_4$)$_2$ hybrid NFs showed excellent operational stability confirming its potential as a biocatalyst in industrial applications. In future works, we intend to study its biocatalytic application to biologically degrade plastics.

Funding

Additional information

No additional information is available for this paper.

CRediT authorship contribution statement

Shamini Anboo: Writing – original draft, Conceptualization. **Sie Yon Lau:** Validation, Supervision, Resources. **Jibrail Kansedo:** Writing – review & editing. **Pow-Seng Yap:** Writing – review & editing. **Tony Hadibarata:** Writing – review & editing. **Azlina Harun Kamaruddin:** Writing – review & editing.

Declaration of competing interest

The authors declare the following financial interests/personal relationships which may be considered as potential competing interests: Sie Yon Lau reports financial support was provided by Malaysia Ministry of Higher Education (FRGS). MyIPo has patent issued to Sie Yon Lau.

Acknowledgements

References

[1] R.C. Kuhad, A. Singh, Biotechnology for Environmental Management and Resource Recovery, 2013, pp. 1–315.
[2] N.J. Turner, Directed evolution drives the next generation of biocatalysts, Nat. Chem. Biol. 5 (8) (2009) 567–573.
[3] S.K.S. Patel, et al., Protein–inorganic hybrid system for efficient his-tagged enzymes immobilization and its application in l-xylulose production, RSC Adv. 7 (6) (2017) 3488–3494.
[4] L. Yu, et al., Fabrication and application of enzyme-incorporated peptide nanotubes, Bioconjugate Chem. 16 (6) (2005) 1484–1487.
[5] S. Anboo, et al., Recent advancements in enzyme-incorporated nanomaterials: synthesis, mechanistic formation, and applications, Biotechnol. Bioeng. 119 (10) (2022) 2609–2638.
[6] P.M.B. Chagas, et al., Immobilized soybean hull peroxidase for the oxidation of phenolic compounds in coffee processing wastewater, Int. J. Biol. Macromol. 81 (2015) 568–575.
[7] J.K.H. Wong, et al., Potential and challenges of enzyme incorporated nanotechnology in dye wastewater treatment: a review, J. Environ. Chem. Eng. 7 (4) (2019).
[8] Z. Temoçin, Covalent immobilization of Candida rugosa lipase on aldehyde functionalized hydrophobic support and the application for synthesis of oleic acid ester, J. Biomater. Sci. Polym. Ed. 24 (14) (2013) 1618–1635.
[9] J. Ge, et al., Recent advances in nanostructured biocatalysts, Biochem. Eng. J. 44 (1) (2009) 53–59.
[10] J. Kim, J.W. Grate, P. Wang, Nanobiocatalysis and its potential applications, Trends Biotechnol. 26 (11) (2008) 639–646.
[11] H. Frenkel-Mullerad, D. Avnir, Sol−gel materials as efficient enzyme protectors: preserving the activity of phosphatases under extreme pH conditions, J. Am. Chem. Soc. 127 (22) (2005) 8077–8081.
[12] H.R. Luckarift, et al., Enzyme immobilization in a biomimetic silica support, Nat. Biotechnol. 22 (2) (2004) 211–213.
[13] J. Ge, J. Lei, R.N. Zare, Protein–inorganic hybrid nanoflowers, Nat. Nanotechnol. 7 (7) (2012) 428–432.
[14] B. Zhang, et al., Preparation of lipase/Zn$_3$(PO$_4$)$_2$ hybrid nanoflower and its catalytic performance as an immobilized enzyme, Chem. Eng. J. 291 (2016) 287–297.
[15] L.-B. Wang, et al., A new nanobiocatalytic system based on allosteric effect with dramatically enhanced enzymatic performance, J. Am. Chem. Soc. 135 (4) (2013) 1272–1275.
[16] L. Zhong, et al., Activated magnetic lipase-inorganic hybrid nanoflowers: a highly active and recyclable nanobiocatalyst for biodiesel production, Renew. Energy 171 (2021) 825–832.
[17] S. Anboo, et al., Synthesis of Enzyme-Based Organic-Inorganic Hybrid Nanoflower Particles, MATEC Web Conf., 2023, p. 377.
[18] B.S. Batule, et al., Ultrafast sonochemical synthesis of protein-inorganic nanoflowers, Int. J. Nanomed. 10 (2015) 137–142 (Special Issue on diverse applications in Nano-Theranostics).
[19] M. Abbas, M. Takahashi, C. Kim, Facile sonochemical synthesis of high-moment magnetite (Fe$_3$O$_4$) nanocube, J. Nanoparticle Res. 15 (1) (2012) 1354.
[20] J. Harris, et al., Hierarchical TiO$_2$ nanoflower photocatalysts with remarkable activity for aqueous methylene blue photo-oxidation, ACS Omega 5 (30) (2020) 18919–18934.
[21] A. Mustafa, A. Karmali, W. Abdelmoez, A sensitive microplate assay for lipase activity measurement using olive oil emulsion substrate: modification of the copper soap colorimetric method, J. Oleo Sci. 65 (9) (2016) 775–784.
[22] S. Lambhiya, G. Patel, U.C. Banerjee, Immobilization of transaminase from Bacillus licheniformis on copper phosphate nanoflowers and its potential application in the kinetic resolution of RS-α-methyl benzyl amine, Bioresour. Bioprocess. 8 (1) (2021) 126.
[23] M. Zhang, et al., Synthesis of catalase-inorganic hybrid nanoflowers via sonication for colorimetric detection of hydrogen peroxide, Enzym. Microb. Technol. 128 (2019) 22–25.
[24] C. Ke, et al., A new lipase–inorganic hybrid nanoflower with enhanced enzyme activity, RSC Adv. 6 (23) (2016) 19413–19416.
[25] S. Li, et al., The 13C amide I band is still sensitive to conformation change when the regular amide I band cannot be distinguished at the typical position in H2O, Chem. Commun. 51 (63) (2015) 12537–12539.
[26] Y. Yu, et al., Self-assembled enzyme–inorganic hybrid nanoflowers and their application to enzyme purification, Colloids Surf. B Biointerfaces 130 (2015) 299–304.
[27] J. Cui, et al., Surfactant-activated lipase hybrid nanoflowers with enhanced enzymatic performance, Sci. Rep. 6 (1) (2016) 27928.
[28] L. Wang, et al., Time-temperature indicators based on lipase@Cu$_3$(PO$_4$)$_2$ hybrid nanoflowers, Lebensm. Wiss. Technol. 168 (2022) 113857.
[29] W. Ren, et al., Synthesis of magnetic nanoflower immobilized lipase and its continuous catalytic application, New J. Chem. 43 (28) (2019) 11082–11090.
[30] A. Teja, P.Y. Koh, Synthesis, properties, and applications of magnetic iron oxide nanoparticles, Prog. Cryst. Growth Char. Mater. 55 (2009) 22–45.
[31] L. Pei, et al., Magnetorheology of a magnetic fluid based on Fe$_3$O$_4$ immobilized SiO$_2$ core–shell nanospheres: experiments and molecular dynamics simulations, RSC Adv. 7 (14) (2017) 8142–8150.

[32] X. Sun, et al., Adsorption mechanism of rhein-coated Fe_3O_4 as magnetic adsorbent based on low-field NMR, Environ. Sci. Pollut. Control Ser. 28 (1) (2021) 1052–1060.

[33] R.J. Hunter, Zeta Potential in Colloid Science: Principles and Applications, vol. 2, Academic press, 2013.

[34] V. Selvamani, Stability studies on nanomaterials used in drugs, in: S.S. Mohapatra, et al. (Eds.), Characterization and Biology of Nanomaterials for Drug Delivery, Elsevier, 2019, pp. 425–444.

[35] F. Matter, A.L. Luna, M. Niederberger, From colloidal dispersions to aerogels: how to master nanoparticle gelation, Nano Today 30 (2020) 100827.

[36] G.W. Lu, P. Gao, Emulsions and microemulsions for topical and transdermal drug delivery, in: V.S. Kulkarni (Ed.), Handbook of Non-invasive Drug Delivery Systems, William Andrew Publishing, Boston, 2010, pp. 59–94.

[37] Z. Zhang, et al., A feasible synthesis of $Mn_3(PO_4)_2$@BSA nanoflowers and its application as the support nanomaterial for Pt catalyst, J. Power Sources 284 (2015) 170–177.

[38] Z. Zhang, et al., Manganese(II) phosphate nanoflowers as electrochemical biosensors for the high-sensitivity detection of ractopamine, Sensor. Actuator. B Chem. 211 (2015) 310–317.

[39] G. Fernández-Lorente, et al., Immobilization of proteins on highly activated glyoxyl supports: dramatic increase of the enzyme stability via multipoint immobilization on pre-existing carriers, Curr. Org. Chem. 19 (17) (2015) 1719–1731.

[40] S. Arana-Peña, et al., Effects of enzyme loading and immobilization conditions on the catalytic features of lipase from Pseudomonas fluorescens immobilized on octyl-agarose beads, Front. Bioeng. Biotechnol. 8 (2020) 36.

[41] C.L. Hawkins, M.J. Davies, Generation and propagation of radical reactions on proteins, Biochim. Biophys. Acta Bioenerg. 1504 (2–3) (2001) 196–219.

[42] K. Li, et al., Carbon nanotube-lipase hybrid nanoflowers with enhanced enzyme activity and enantioselectivity, J. Biotechnol. 281 (2018) 87–98.